

Local Operational Geomagnetic Index K Calculation (K-LOGIC) from digital ground-based magnetic measurements

Authors:	Stan Stankov	RMI	S.Stankov@meteo.be
	Koen Stegen	RMI	K.Stegen@meteo.be
	Rene Warnant	RMI	R.Warnant@meteo.be
Release:	1.1	01.10.2010	Unclassified

DISCLAIMER

All efforts have been made to ensure accuracy of the content of this report. However, the user assumes the entire risk related to the use of the information -- research, developments, and/or data -- presented in this report. The author/s and RMI disclaim any and all warranties, whether express or implied, including (without limitation) any implied warranties of merchantability or fitness for a particular purpose. In no event will the author/s and RMI be liable to you or to any third party for any direct, indirect, incidental, consequential, special or exemplary damages or lost profit resulting from any use or misuse of the information in this report. All rights reserved.



STR-RMI-2010-01	Unclassified	Version: 1.1 / 01.10.2010	Page: 2 / 32
Title:	Local operational geomagnetic index K calculation (K-LOGIC) from digital ground-based magnetic measurements		

DOCUMENT CHANGE RECORD

VERSION	DATE	CHANGE RECORD	AUTHOR
0.1	01.01. 2010	First Draft	S. Stankov
1.0	01.08.2010	First Version	S. Stankov
1.1	01.10.2010	Evaluation results added	S. Stankov

SUMMARY

A nowcast system for operational estimation of a proxy, K-type, geomagnetic index (K index) is presented. The system is based on a fully automated computer procedure for real-time digital magnetogram data acquisition, screening the dataset and removing the outliers, estimating the solar regular (S_R) variation of the geomagnetic field, calculating the K index, and issuing an alert if storm-level activity is indicated. This is a time-controlled (rather than event-driven) system delivering as regular output: the K value, the estimated quality flag, and eventually, an alert. Novel features are first, the strict control of the data input and processing and second, the increased frequency of producing the index (every one hour). Such quality control and increased time resolution have been found to be of crucial importance in various applications, e.g. ionospheric monitoring, that are of particular interest to us and to users of our service. The nowcast system operability, accuracy and precision have been tested with instantaneous measurements from the recent years. A statistical comparison between nowcast and definitive index values proves that the average r.m.s. error is smaller than 1 K unit. The system is now operational at the site of the RMI Geophysical Centre in Dourbes (50.1°N, 4.6°E) and is being utilised for alerting users when geomagnetic storms take place.

ACKNOWLEDGEMENTS

The authors thank J. Rasson and I. Kutiev for the helpful discussions, and J. L. Marin for the technical support. This work is supported by the Royal Meteorological Institute via grant GJU/06/2423/CTR/GALOCAD and the RMI Solar-Terrestrial Centre of Excellence (STCE). The results presented in this report rely on data collected at magnetic observatories -- thanks are due to the national institutes that support these observatories and INTERMAGNET (www.intermagnet.org) for promoting high standards of magnetic observatory practice.



STR-RMI-2010-01	Unclassified	Version: 1.1 / 01.10.2010	Page: 3 / 32
Title:	Local operational geomagnetic index K calculation (K-LOGIC) from digital ground-based magnetic measurements		

TABLE OF CONTENTS

1. INTRODUCTION	4
2. THE GEOMAGNETIC FIELD – ORIGIN, OBSERVATION, VARIABILITY, AND DESCRIPTIVE K-INDICES.....	6
3. ALGORITHM FOR K INDEX CALCULATION BASED ON THE LINEAR ELIMINATION METHOD	10
4. ALGORITHM FOR REAL TIME K INDEX CALCULATION	12
5. K INDEX NOWCAST SYSTEM AT A SINGLE OBSERVATION SITE - DEVELOPMENT.....	20
6. K INDEX NOWCAST SYSTEM – ASSESSMENT OF PERFORMANCE.....	22
7. SUMMARY AND OUTLOOK.....	26
REFERENCES.....	29

1. Introduction

There is an ongoing demand for services that can provide real-time assessment of the (global and local) geomagnetic activity and identified as being of importance to space weather research and modelling, exploration geophysics, radio communications, satellite-based positioning/navigation, etc. (*Kohl et al.*, 1996; *Datta-Barua et al.*, 2005; *Burger et al.*, 2006; *Stankov et al.*, 2006, 2009; *Stankov and Jakowski*, 2007; *Warnant et al.*, 2007a, 2007b, 2007c; and the references therein). Monitoring services depend largely on the reduction of solar and geomagnetic observations to generate reliable indices of activity. There are several internationally-recognised indices that are currently in use, some of the most widely used being the K indices (*Bartels et al.*, 1939; *Chapman and Bartels*, 1940; *Knecht*, 1972; *Mayaud*, 1980; *Jacobs*, 1987; *Menvielle and Berthelier*, 1991; *Siebert*, 1996). The K index is a quasi-logarithmic index characterising the 3-hourly range in transient magnetic activity relative to the regular “quiet-day” activity for a single site location. K-derived planetary indices, such as Kp or am, that are derived from K indices measured at a planetary network of geomagnetic observatories, provide convenient measures of the global geomagnetic activity. Despite their imperfections, these planetary geomagnetic indices are much used in the upper atmosphere science together with the solar activity indices -- the solar sunspot number (Rz) and the solar 10.7 cm radio flux index (F10.7) (*Akasofu and Chapman*, 1972).

Originally, the K index was scaled manually (*Mayaud*, 1967) from analogue (photographic) magnetograms with a standard recording speed of about 20 mm per hour. With the advances of electronic equipment and computer technologies however, the data acquisition and processing, plus the consecutive production of the K index, have gradually shifted into utilising these new (digital) technologies (*Van Wijk and Nagtegaal*, 1977; *Niblett et al.*, 1984; *Riddick and Stuart*, 1984; *Hopgood*, 1986; *Wilson*, 1987; *Menvielle*, 1990). Several computer-based methods for calculating the K indices were developed along the way (*Jankowski et al.*, 1988; *Pirjola et al.*, 1990; *Sucksdorff et al.*, 1991; *Nowozynsky et al.*, 1991; *Menvielle et al.*, 1995; and the references therein). Following a thorough examination with the help of manually scaled indices (*Menvielle et al.*, 1995; *Bitterly et al.*, 1996), it has been found that the method of linear elimination (a.k.a. the FMI/Finnish method) delivers the best results and, also very important, is directly applicable for any observatory.

While the computer-based derivation of the K indices was a major step towards higher operational efficiency and lower costs, the nowcast, i.e. the automated data acquisition and processing together with the geomagnetic activity index production in real time, is now mandatory for the variety of space weather services being developed around the world (*Berthelier et al.*, 1996; *Takahashi et al.*, 2001; *Andonov et al.*, 2004; *Wing et al.*, 2005; *Viljanen et al.*, 2008). However, there are several important issues related to geomagnetic indices production. Although the 3-hour K-derived planetary geomagnetic index played a basic role in geomagnetism and aeronomy for a very long time, and is still a good representation of the large-scale geomagnetic and ionospheric disturbances, it appears to be not accurate enough when representing disturbances of a smaller scale. From this perspective, the local K index (derived from the nearest magnetic station/s) fits the observations of small-scale disturbances better than the global K-derived planetary index and might be considered as a better choice. Moreover, the 3-hour interval between two consecutive indices determination is much larger than the shorter characteristic time of localised ionospheric phenomena and effects on GNSS applications that are of particular interest to us.

The purpose of this report is to present an experience in developing a nowcast system for local operational K-type geomagnetic index calculation (K-LOGIC) that addresses the above-mentioned issues. K-LOGIC complements our previous and ongoing developments in space weather monitoring at the Royal Meteorological Institute's (RMI) Geophysical Centre in Dourbes (50.1°N, 4.6°E) (*Jodogne and Stankov, 2002; Stankov et al., 2004; Warnant et al., 2007a*). However, since the proposed nowcast index does not strictly follow the calculation of the K index as defined by *Bartels et al. (1939)*, it should be referred as a proxy, K-type index. Nevertheless, in this report it will be referred simply as 'K index'.

The report is organised as follows. First, the geomagnetic field's origin and activity, related observations and descriptive indices will be briefly reviewed. Next, one of the most popular procedures for K index calculation will be described. After that, the algorithm for real-time index calculation will be detailed, followed by description of the K-LOGIC system developed at the RMI Geophysical Centre. A (preliminary) assessment of the system performance is made in the next section. Finally, the results are discussed in view of further developments and applications.

2. The geomagnetic field – origin, observation, variability, and descriptive K-indices

The geomagnetic field is generated within the Earth's core through a complex combination of the Earth's daily rotation, thermal movements, and electrical currents within the core (*Jacobs, 1987; Olsen et al., 2007*). Thus, a giant dynamo is formed that sustains a magnetic field very similar to that of a bar magnet slightly inclined to a line that joins the North and South geographic poles. The Earth's magnetic field is subjected to the solar wind (a fast moving stream of charged particles, electrons and protons, ejected from the upper atmosphere of the Sun) that envelopes the Earth's magnetic field, flattening the field lines on the sun-ward side and stretching them out on the opposite side. The total field intensity (F) can be divided into several components (**Fig.1**).

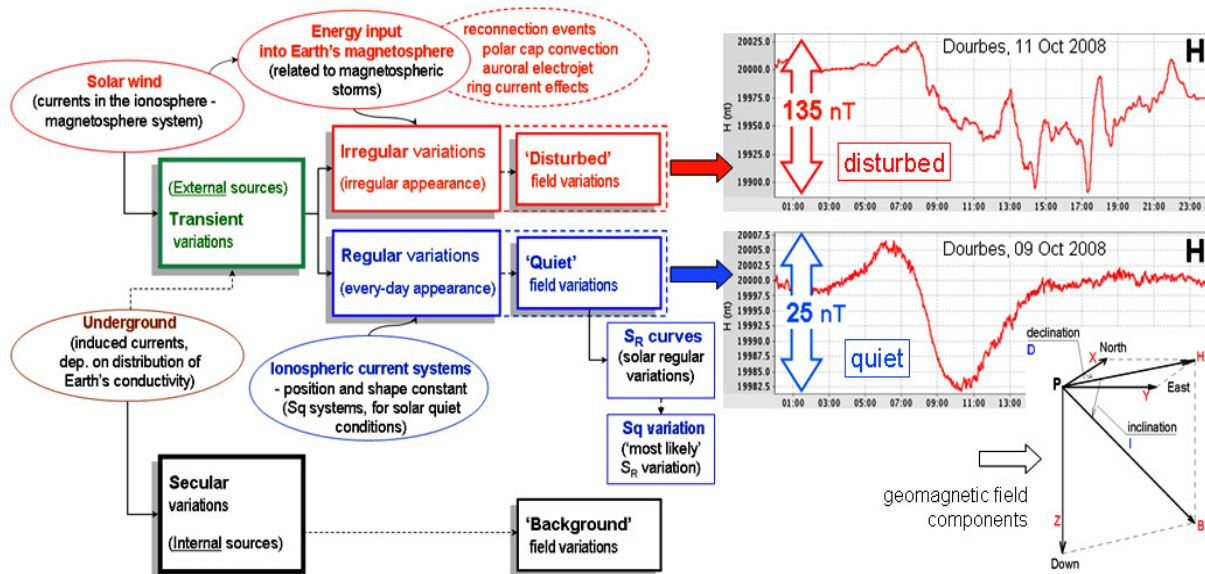


Fig.1. Geomagnetic field components and variations – secular/transient, regular/irregular and quiet/disturbed (after *Menvielle and Berthelier, 1991; Siebert, 1996*).

The declination (D) indicates the difference between the headings of geographic north and magnetic north, while the inclination (I) is the angle of the magnetic field above/below horizontal. The horizontal intensity (H) defines the horizontal component and the vertical intensity (Z) defines the vertical component of the total field intensity. If any three of the above components are available, the rest of them can be determined from the following formulae (*Chapman and Bartels, 1940; Knecht, 1972; Jankowski and Sucksdorff, 1996*):

$$\begin{aligned}
 B^2 &= X^2 + Y^2 + Z^2 = H^2 + Z^2 \\
 H^2 &= X^2 + Y^2 \\
 X &= H \cdot \cos D \\
 Y &= H \cdot \sin D = X \cdot \tan D \\
 Z &= B \cdot \sin I = H \cdot \tan I \\
 D &= \arctan(Y/X) \\
 I &= \arctan(Z/H)
 \end{aligned}$$

The geomagnetic field experiences pronounced variations that are the sum of the secular variations (whose sources are mostly internal) and the transient variations (whose sources are external) (**Fig.1**). The secular variations are very slow in opposite to the transient variations that are of prime interest to us.

The main purpose of the geomagnetic activity indices is to quantify the degree of the geomagnetic field disturbance (local or global) and to characterise the origin and time scale of the field variations. There are two major types of geomagnetic indices: on the one hand, indices that separate and quantify the variations representative of a localised/isolated effect (e.g. Dst for the ring current variations) and indices that estimate the global energy input in the magnetosphere, which is the purpose of the so-called “planetary” indices (e.g. Kp and Ap).

The K index accounts for the morphological characteristics of the transient irregular variations and is designed to characterise the geomagnetic activity during a 3-hour interval at a certain location. The 3-hour duration of the interval stem from morphological considerations and the same 3-hour (UT) intervals (00-03, 03-06, 06-09, 09-12, 12-15, 15-18, 18-21, 21-24) are used at any station where K indices are produced. These intervals are long enough to correctly account for certain perturbations of one or two hours in duration (e.g. bays) and, at the same time, are short enough not to affect too much of the daily index when such short-term disturbances happen to occur over 2 consecutive intervals (*Menvielle et al., 1995*).

The K index is derived from the amplitude of the variations of the field’s horizontal components (the H and D pair, or alternatively, the X and Y components) after subtracting the daily solar regular (S_R) variation for the particular component (cf. **Fig.2**).

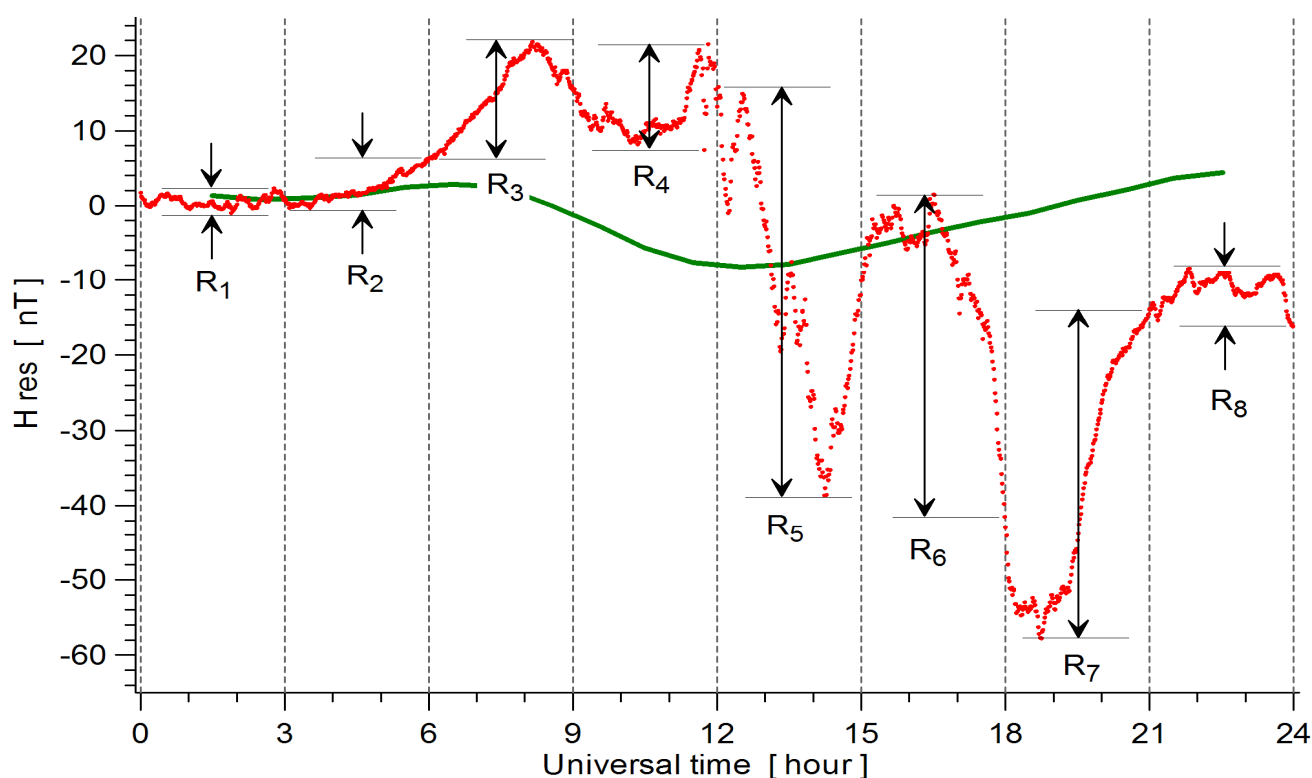


Fig.2. Calculation of the 3-hour K index over a 24 hour period. A daily record of 1-min measurements of the H component is presented here to illustrate the elimination of the solar regular variation, the S_R curve (the solid line), and the consequent determination of the 8 ranges ($R_i, i=1,8$). The difference between the upper (maximum) and lower (minimum) envelopes that are parallel to the S_R curve, determines the disturbance range within every 3-hour interval.

The K index is an integer number between 0 (indicating ‘very quiet’ geomagnetic field) and 9 (‘very disturbed’ geomagnetic field), corresponding to the larger of the two ranges measured in the field’s horizontal components over the specified 3-hour period. In fact, the K index is a code, and although expressed in integers, it refers to a level (“class”) on a quasi-logarithmic scale consisting of 10 gradually increasing ranges (**Table I**).

K-index value	Limits of Range Classes, nT (Niemegek)	Limits of Range Classes, nT (Dourbes)	Limits of Range Classes, nT (Manhay)
0	0 - 5	0 - 4.9	0 - 4.9
1	5 - 10	4.9 - 9.7	4.9 - 9.7
2	10 - 20	9.7 - 19.4	9.7 - 19.4
3	20 - 40	19.4 - 38.9	19.4 - 38.9
4	40 - 70	38.9 - 68.0	38.9 - 68.0
5	70 - 120	68.0 - 116.6	68.0 - 116.6
6	120 - 200	116.6 - 194.4	116.6 - 194.4
7	200 - 330	194.4 - 320.8	194.4 - 320.8
8	330 - 500	320.8 - 483.0	320.8 - 483.0
9	500 +	483 +	483 +

Table I. Limits of range classes (expressed in nT) for the K index, for the reference Niemegek observatory (NGK, 52.1°N, 12.7°E) and the two Belgian observatories, Dourbes (50.1°N, 4.6°E) and Manhay (50.3°N, 5.7°E).

In practice, the actual calculation of the 3-hour K index is done in the following manner. First, the non-K variations need to be eliminated. For the purpose, the solar regular (S_R curve) is established from the quietest days of the season, usually, the 5 quietest days in the current month are used. After that, for every 3-hour (UT) interval, two parallel curves are plotted, limiting (touching) the actual trace of the field component from below and from above. The vertical difference between the two curves, is the range R_i for the respective 3-hour interval (t_i , $i=1,8$) of the day. The range R_i is then converted to the corresponding K index according to a 10-step quasi-logarithmic scale (**Table I**). The scale is strictly logarithmic up to the value of $K=3$, i.e. the range limits increase by a factor of two. For higher values of K however, the increase of the range limits was set less steep because otherwise the occurrence frequency of top values $K=7,8,9$ would have been far too small for a reasonable statistical evaluation (*Siebert, 1996*).

In general, the intensity of the geomagnetic perturbations increases from the geomagnetic equator towards the auroral zone on each hemisphere, so each geomagnetic observatory needs to define its own table assigning K from the measured ranges (R_i). In practice, all tables contain simply multiples of the range limits for Niemegek. Since the scale is logarithmic, it is sufficient for a given observatory to establish/indicate the lower limit for $K=9$ only and the rest of the limits are then easily obtained. For example, in the case of Dourbes (DOU), the lower limit for $K=9$ is $R_{lim,9}^{DOU} = 486$ nT, so having the range limits for Niemegek $R_{lim,i}^{NGK}$ (Table I) it is easy to obtain the corresponding range limits for Dourbes using the formula:

$$R_{lim,i}^{DOU} = R_{lim,9}^{DOU} \times R_{lim,i}^{NGK} / R_{lim,9}^{NGK}, \quad i = 0, 1, 2, \dots, 8, 9.$$

The limits of range classes for the reference Niemegek observatory and the two Belgian observatories, Dourbes (DOU) and Manhay (MAB) are provided in **Table I**.

The guiding principle when specifying the limits of range classes is the assimilation of frequency curves. It has been found that for each station, in a sufficiently long time interval, there should be about the same occurrence frequency for any K index.

A derivative (mean standardized K index), so-called “planetary” K index (Kp) is also defined, based on the ranges of variation within the 3-hour periods observed in the records from several selected geomagnetic observatories (currently 13) located at sub-auroral latitudes (i.e. between about 45 degrees and 65 degrees). After weighting and averaging of the local K indices, the standardised mean Kp value for every 3 hours of the day is obtained again on the same quasi-logarithmic scale but in addition to the original 10 integers, additional intermediate values containing one and two thirds of a K unit (KU) are introduced by use of the symbols ‘+’ and ‘-’, thus having now 28 Kp values in total: 0, 1-, 1, 1+, 2-, 2, 2+, 3-, ... , 7+, 8-, 8, 8+, 9-, 9.

While the 3-hour planetary Kp index played a basic role in geomagnetism and aeronomy for a very long time, and is still a good representation of the large-scale ionospheric disturbances (ionospheric storms), it appears to be not accurate enough when representing ionospheric disturbances of a smaller scale. The small-scale disturbances are localised phenomena and the local K index, derived from the nearest magnetic station, fits the observation of these disturbances better than the global, Kp index. Moreover, the 3-hour time scale is much larger than the shorter characteristic time of small-scale ionospheric variations.

3. Algorithm for K index calculation based on the linear elimination method

Several approaches to the computer derivation of the K index from digital records have been proposed during the years, which fall into four major categories (*Menvielle et al.*, 1995; and the references therein): regression over a sliding windows (successively centred on every hour of the day), regression with further constraints, frequency filtering of magnetograms, and decomposition based on orthogonal vectors. Following a thorough evaluation against hand-scaled K indices by using a common data set and performing the same statistical tests (*Menvielle et al.*, 1995), it has been found that the linear elimination (a.k.a. FMI) method (*Sucksdorff et al.*, 1991) delivers the best results and, also very important, is directly applicable to any observatory. The principal difficulty in determination of the K index is the establishment of the regular solar diurnal variation (S_R), which is used as a reference from which the K variations are scaled (*Hopgood*, 1986; *Walker*, 1987). Here we will outline the FMI algorithm (**Fig.3**) that will be used in our post-processing module for determining the “close-to-definitive” K value.

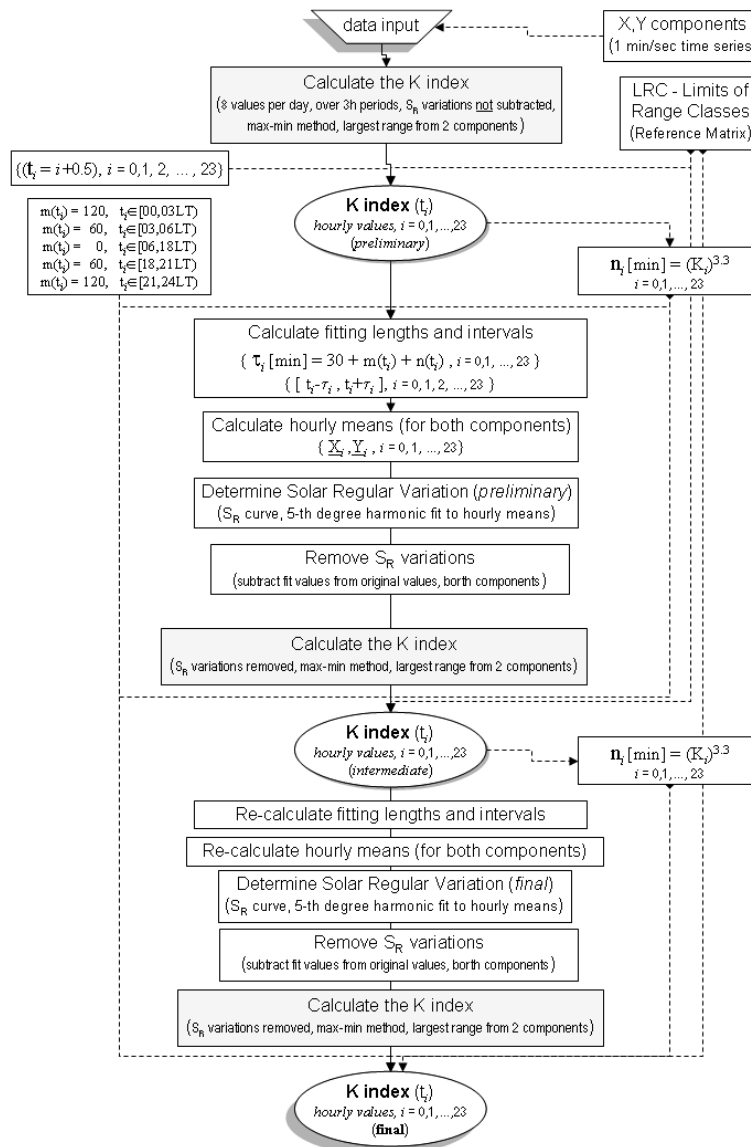


Fig.3. The K index calculation based on the linear elimination algorithm (after *Sucksdorff et al.*, 1991).

The FMI approach is applicable for calculating the standard 8 values of K for any given day as long as measurements from both, the preceding and the following day, are available. It uses 1-minute (or denser) digital magnetogram records of the X and Y components. It should be underlined that, although the algorithm is suitable for any geomagnetic observatory, the magnetic field variations depend on location (the geomagnetic latitude in particular), therefore the limits of range classes (**Table I**) need to be adjusted a priori for each observatory.

In a preliminary step of the algorithm, the data gaps are filled via linear interpolation, provided that gap lengths do not exceed a certain pre-defined threshold. In the next step, the 8 preliminary K values are obtained (for the 3-hour intervals) by applying the simple “max-min” method (i.e. by calculating the difference between the component’s maximum and minimum within the predefined time interval) and then selecting the larger of the two horizontal components’ ranges. Such K values are preliminary because, at this stage, the S_R variations are not available and hence, not possible to remove from the original data records. The 24 hourly values of K are obtained by assuming that, in each 3-hour interval, the 1-hour K values for each of the three hour-long subintervals are the same.

The next major task in the procedure is to determine the S_R variation curve. For the purpose, the hourly means of each component are calculated from the data of that hour plus the data from the two neighbouring time periods, each of length of $m+n$ minutes. The number m depends on the local time: $m = 0$ during daytime hours (06-18LT), $m = 60$ during dawn (03-06LT) and dusk (18-21LT), and $m = 120$ during night (21-03LT). The number n depends on the geomagnetic activity at that hour ($n = K^{3.3}$), where K is the preliminary value from the previous step. Having calculated the mean values (assigned to the middle points of each hour) of a component for each of the 24 hours, a 5-th degree harmonic fit to these values is performed and the S_R curve for that particular component is thus established. These approximated values are then subtracted from the original magnetogram values of the component. Having the S_R variations removed from the original data of both horizontal components, the intermediate K values are derived by applying the max-min method and selecting the larger of the two horizontal components’ ranges.

In the final step, the intermediate K values are used for determining a refined S_R curve in the same manner as in the previous step. In doing so, the fitting lengths and intervals are re-defined using the intermediate K values, the hourly means are re-calculated and the new, final S_R curve is produced (again, by applying a 5-th degree harmonic fit to the re-calculated hourly means). After removing the regular variations from the original data, the final K index values are determined.

4. Algorithm for real time K index calculation

Since the FMI method relies on data from the following day, it is obvious that we cannot directly implement this method for real time calculation unless some modifications are implemented. There are two major issues associated with that – one is the 3-hour intervals used for the index calculation and the other is the establishment of the S_R variation curve.

In the general practice, the standard 3-hour time intervals however, for our applications we need a K value produced at least once every hour. This raises the question of whether the hourly K values derived from data within only 1-hour intervals differ from the conventional 3-hour K values and to what extent. There are also concerns about the possible difference in physical processes reflected by the 3-h index versus the shorter time interval indices. It has been shown (*Della-Rose et al., 1999*) that the index estimation based on the same methodology but with different time windows, ranging from 15 min to 5 hours, results in considerably different K index values. To avoid this uncertainty, we calculate the K index with data from a 3-hour period (window), but sliding this window with 1-hour steps, thus producing a K value each hour based on the preceding 3 hours of data. The K value at each step is assigned to the window's end.

The second issue, the establishment of the S_R variation curve, requires substantial analysis based on data from up to a month-long time series ending at the current moment. Quiet days are defined as the days in which the preliminary $K < 3$ and the S_R curve is established from these days only.

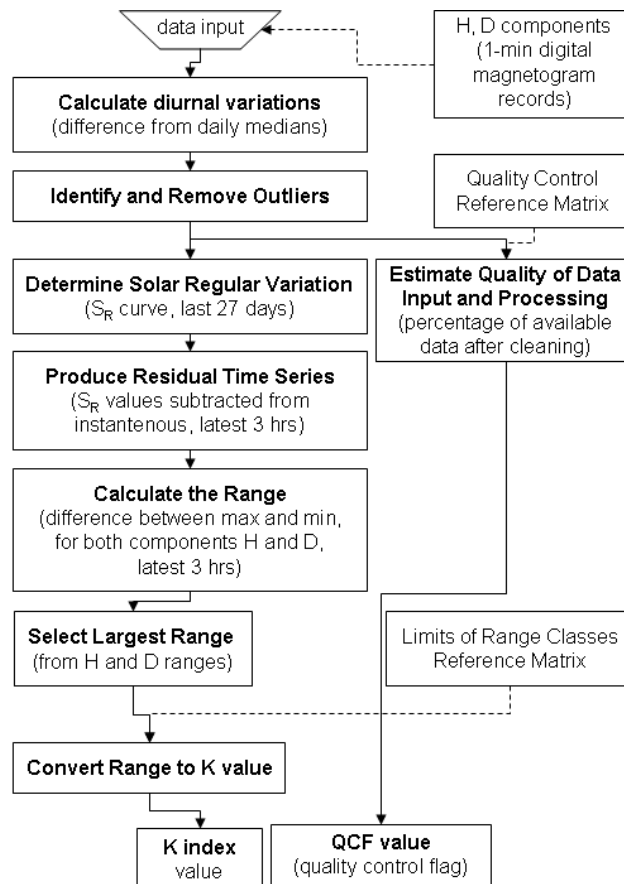


Fig.4. Schematic of the algorithm for real-time calculation of the K index.

4.1 Algorithm outline

Following on the principles of real-time computing (*Mellichamp, 1983; Heitmeyer and Mandrioli, 1996*), the algorithm (**Fig.4**) was designed to be easily maintained, adaptable to different observatories, and to fulfil the following tasks: input data screening and cleaning, establishment of the S_R variation curve, actual K index calculation, and quality control of data input and processing. Every single K value is assigned a quality flag and, depending on this flag and the purpose of using the index, the value can be either accepted or ignored.

4.2 Data pre-processing (screening and cleaning)

A common problem associated with the digital magnetometer data acquisition is the presence of noise, data gaps and spurious non-physical data values (outliers/spikes). Such anomalous records stem from various technicalities, most frequent being the degradation in instrument precision due to external factors. The problem has two aspects – the timely identification and the handling of these technicalities. Defining such “bad” records is a substantial problem by itself that depends strongly on the nature of the observed physical characteristics, in this case the geomagnetic field components. Handling the bad record data depends on the purpose of using the measurements – a highly-accurate product from best quality data only or a best guess from even poorly sampled data. In the former case the bad records are discarded (and production is abandoned if the bad record length exceeds a certain threshold) while in the latter case the records are usually “repaired” by some sort of approximation and the production may continue. Both, identifying and handling bad records becomes even a greater challenge when needed to be done in real-time, while the subsequent data keeps flowing in and a higher level product (e.g. index and/or alert) needs to be generated rather promptly.

An outlier (spike) is defined as a data instance/observation that appears to deviate markedly from other members of the sample/population, in other words is far outside the norm for a variable or sample/population (*Bevington, 1969; Grubbs, 1969; Swaroop, 1971; Snedegor and Cochran, 1980; Schultz and Zhang, 1990*). Outliers, being the most extreme observations, will include the sample maximum or minimum, or both; however, the maximum and/or minimum need not be outliers as long as they are not unusually far from other observations. The concept of the “fringelier” was also introduced, referring to an unusual event occurring more often than seldom. Such fringeliers may extend well over two standard deviations from the mean and may have a disproportionately strong influence on parameter estimates, but yet are not easily identified as typical outliers due to their relative proximity to the distribution centre. As fringeliers are a special case of outliers we will use both terms interchangeably. In magnetogram records the gaps/outliers usually occur in isolation (**Fig.5A**) or in small clusters (**Fig.5B,C**), however there are cases when occurrence can be more often and for a prolonged period of time (**Fig.5D**). The latter case (**Fig.5D**) is typical when there is a substantial degradation in the instrument’s operation/precision due to external influences, such as problems with the electrical supply or “cultural noise”. The presence of outliers in data samples can lead to inflated error rates and/or substantial distortions of parameter and statistical estimates.

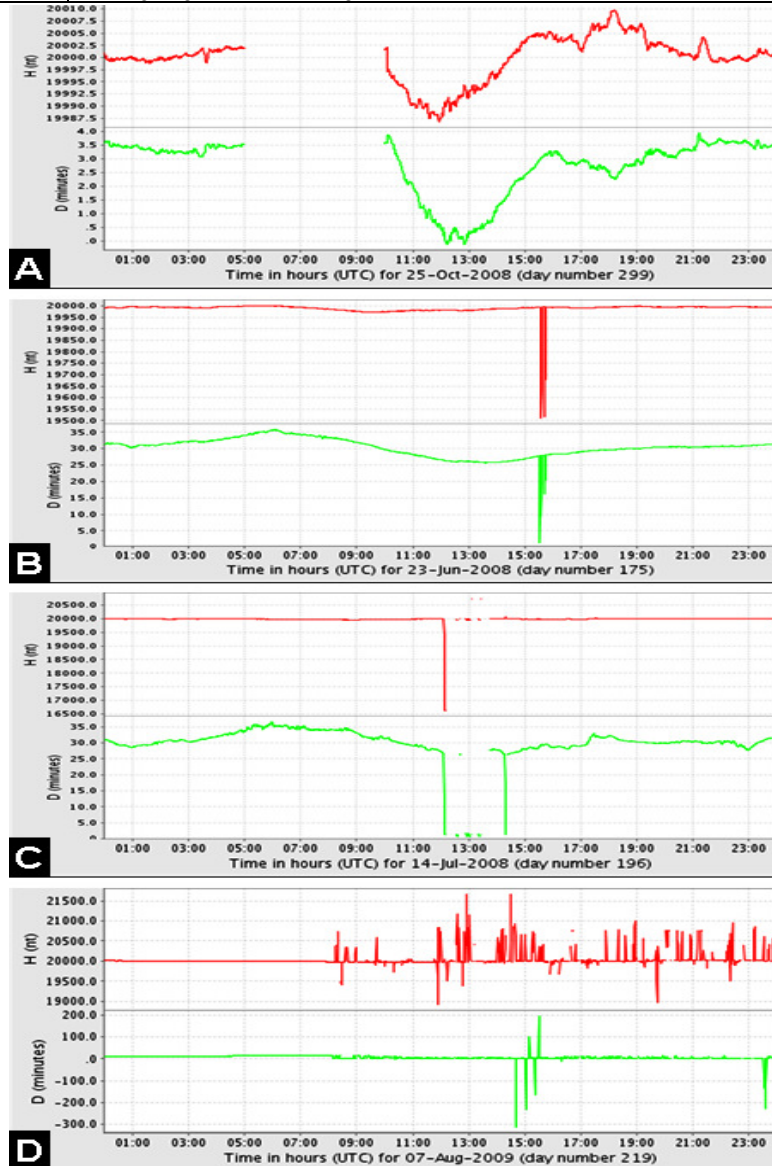
Title: Local operational geomagnetic index K calculation (K-LOGIC)
 from digital ground-based magnetic measurements


Fig.5. Identification of gaps and spurious/noisy data. Panel (A): Data gap. (B): Cluster of outliers. (C): Data gap accompanied with outliers and regular data. (D): Sustained occurrence of noisy data due to technical problems.

Bad data are dealt with by calculating the standard deviation of the latest 3-hour long data sample (1-min measurement records of the geomagnetic field components) that enters the algorithm, but only after removing the median diurnal variations. In our procedure, the number of standard deviations (σ) from the local means that define a spike is set to 2.5σ . The spikes are then discarded (no interpolation allowed) and their position is treated as a gap. Different limits were tested and it was found that the imposed $\pm 2.5\sigma$ limits discard the majority of bad data points while not rejecting naturally caused perturbations. A more complicated approach may include wavelet analysis directly applicable to magnetograms (*Mendes et al., 2005*). As a precaution, the maximal number of consecutive data points considered a single spike event is set to 5 (i.e. in the time domain, given the 1-min resolution, a spike should not extend longer than 5 minutes). In case of a longer-lasting irregularity, the latter is treated as a sequence of spikes. Also, hard flag threshold for the maximal number of spikes is set to 10%. Nevertheless, the above thresholds are not to be considered as ultimate, their choice depends on the error that can be tolerated in the final product.

4.3 Determination of the solar regular variation (S_R) curve

The establishment of the current 24-hour solar regular (S_R) variation in a given geomagnetic field component is one of the key modules in the K index calculation procedure. Obtaining the S_R curve in real time by directly applying the FMI method is impossible because it requires data measurements from a variable-length time period extending on both sides of the current moment in time. In case of increased geomagnetic activity, the interval may extend for several hours in the future. There is a way around this obstacle, for example to apply the method using data up to the immediate past which obviously comes at the expense of accuracy. Alternatively, assuming that the S_R curve is slowly changing from day to day, it is possible to select the magnetically quietest days in the most recent month and after calculating the monthly medians for each hour of the day to derive an approximation suitable for use as a “quiet-day-curve” (e.g. *Takahashi et al.*, 2001). We have adopted a similar approach based on measurements from the latest 27-day period. The derivation of the S_R curves will be demonstrated next with actual measurements from the Dourbes geomagnetic observatory (cf. **Fig.6**).

Fig.6G shows the raw 1-min measurement values of the H component as recorded during the months of March, June, and December 2008. For reference only, the definitive Kp and Dst indices are plotted in the bottom panels, **Fig.6H**. **Fig.6F** shows the superposed 1-day plots of the H component. Large perturbations, detected during disturbed magnetic conditions, are clearly visible. The calculated hourly medians, means and the corresponding standard deviations are plotted in **Fig.6E**. Patterns in the daily variations already appear, with generally lower values observed in the morning hours. The cases of large differences observed between the medians and the means stem from the presence of bad data points that affect the calculation of both the means and the standard deviations.

In order to eliminate the secular geomagnetic variation, the daily median value of the H component has been calculated and then subtracted from the original records for each day to obtain the relative deviations (**Fig.6D**). Next, measurements from the quiet geomagnetic days only (i.e. the 3-hour Kp index never reaching a value of 3 during these particular days of the 27-day period) have been selected and the corresponding measurements plotted after cleaning bad data (**Fig.6C**). The data dispersion is now much smaller (**Fig.6B**); however, it should be noted that the diurnal trend in both the all-Kp and the low-Kp cases is well established and similar. The calculated median values are actually the anchor points of the S_R curve we need to determine. Medians are used instead of means because the latter are sensitive to bad data and we try to eliminate any possibility of the procedure being compromised. Approximation (based on the medians) is needed if we want to obtain S_R values at 1-min steps. The S_R curve itself is obtained after applying a simple polynomial approximation (**Fig.6A**); however, Fourier transform, cubic spline, Chebyshev, or other approximations are possible alternatives.

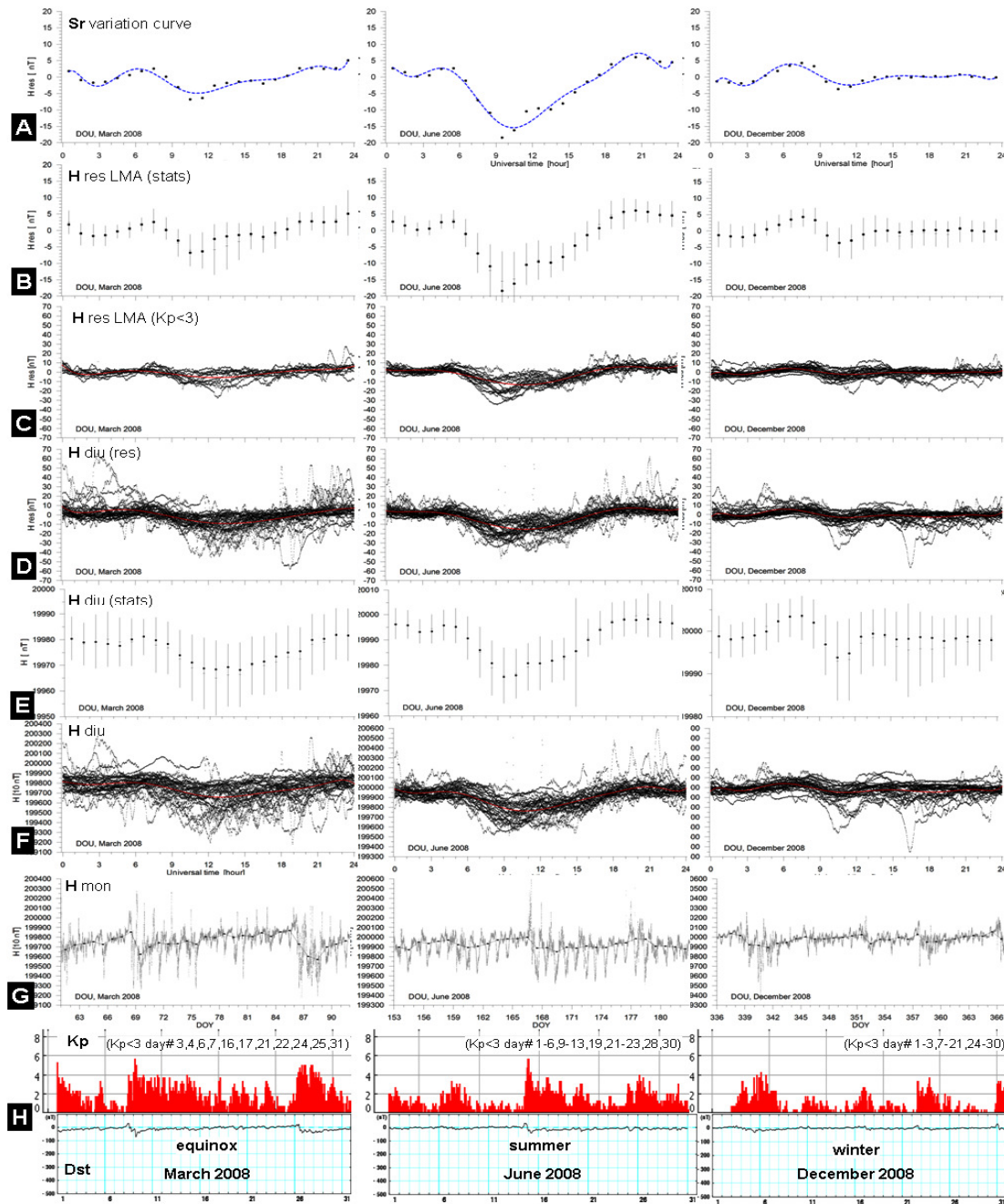


Fig.6. The S_R curve establishment from 1-min measurements of the H component from observations at Dourbes during equinox (left panels), summer (middle), and winter (right) months. Bottom panel (H) shows the global geomagnetic activity as described by the Kp and Dst indices. (G): Real-time 1-min measurements of the H component. (F): The superposed diurnal variations. (E): Median (solid circles), mean (–) and standard deviations (vertical bars) of the diurnal variations. (D): Diurnal variations (relative) with daily medians removed. (C): Diurnal variations (relative, cleaned) from quiet days ($K_p < 3$) only. (B): Median (solid circles), mean (–) and standard deviations (vertical bars) of the diurnal variations (relative, quiet-days). (A): The S_R curve (polynomial approximation) based on the median diurnal relative quiet-day variations.

It is obvious how the S_R variations change with season, with the largest daily amplitude observed in the summer. This fact requires that, in a nowcast service, the established S_R curve is updated on a regular basis, at least once a month. It should be noted that the S_R curve pattern differs from station to station, especially when different stations are located at different magnetic latitudes.

4.4 K index calculation

The actual K index calculation is performed only after the data has been cleaned and the S_R curve established from past records. Having determined the S_R approximation values, the regular diurnal variations (represented by this approximation) are then subtracted from the corresponding 1-min measurements of the horizontal (H and D) components (**Fig.7A**). In this way, the calculated residuals are ready for determination of the ranges, i.e. the component's maximum value minus the minimum value within every 3-hour interval. After determining the ranges, their conversion into a K index value (**Fig.7B**) is straightforward given the LRC (limits-of-range-classes) table (**Table I**). The K value at each step is assigned to the window's end.

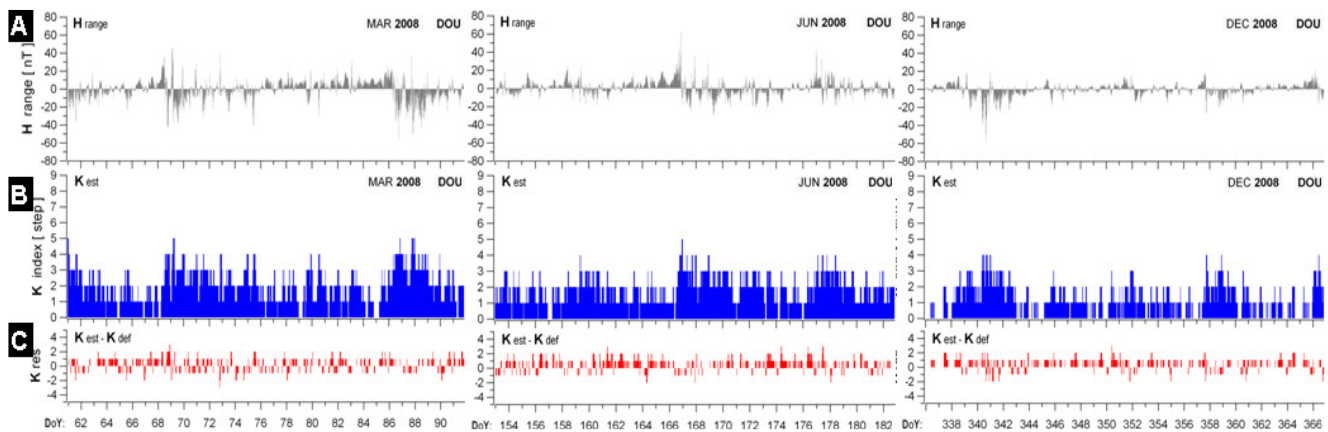


Fig.7. Results of the K index nowcast (panels B) together with the corresponding residual errors, i.e. nowcast minus definitive values (panels C) for the months of March, June, and December 2008 as produced from the observations at Dourbes. The top panels (A) display the observed H component's deviations from the S_R curve.

As an example, presented here are results of the K index calculations (**Fig.7**) during March, June, and December 2008 for the Dourbes observatory. A quick comparison with the definitive K values is also provided (**Fig.7C**). We used a sliding window of 3 hours, so a K index value is obtained every 1 hour but based on data from the latest 3 hours. The RMS (root-mean-square) error is around 1 KU, being generally larger during increased geomagnetic activity.

More details are presented in the section about the nowcast system performance assessment.

4.5 *Quality control*

As mentioned earlier, our objective is to develop a nowcast service that will be able to produce the K index for further use in higher-level products such as alerts/warnings to be promptly dispatched to users when the index value suggests the presence of active/storm geomagnetic conditions. Hence, the definitive K value is not the (sole) purpose of the here-presented procedure. Nevertheless, the procedure should be developed in such a way as to ensure the best possible outcome, i.e. a nowcast value as close as possible to the definitive value. From this perspective, it is necessary to have a quality control (QC) system, capable of immediately assessing the input dataset quality and the nowcast output, i.e. the K index value. Naturally, the immediate assessment of K is a challenge because a highly-reliable “close-to-definitive” value of K can be produced not earlier than several hours (even days) in future. By then however, the current nowcast value will be practically useless for the purpose of alerting the users. Therefore we need to perform quality control based on the information available up to the current moment only.

The key concept of the implemented QC system is based on the expectation that a complete and sound dataset would provide the ideal platform for a top quality, reliable, closest-to-definitive value of the K index. In this sense, any gap in the data buffer (i.e. the 3-hour-long record currently used for calculating the K value) would erode the quality of the produced output. Furthermore, the time elapsed since the occurrence of the latest gap is crucial. For example, if a nowcast system is developed with time resolution of 1 hour (i.e. the nowcast run every one hour) and there is no data coming in from the last hour, there is not much sense in producing a new K value at this moment because it would be effectively a delayed (by 1 hour) forecast rather than a nowcast. Therefore, the QC system should reflect on both, the total length of data gaps (shorter or no gaps – the better) and the time elapsed from the latest gap (more distant the gap in the past – the better).

The extent of data cleaning (treatment of outliers in particular) should also be included in the QC system. Here, the outliers are removed from the input dataset (note: an alternative approach is to try interpolation) and are, ultimately, treated as gaps. In this way, handling the outliers is translated into handling data gaps only, which substantially facilitates the QC system. In the nowcast algorithm, the first QC estimation follows the data screening (gaps identification and removal of outliers).

In summary, the currently implemented quality control system (cf. **Table II**) provides an estimation of the confidence put on the produced nowcast K value.

QCF (numeric)	QCF (verbose)	Description	Output availability
10	nominal	<i>Top (highest) quality, complete & sound input dataset (no gaps, no outliers, no problems of any sort encountered during data screening and processing)</i>	yes
9	very good	<i>High quality, 100% (latest 1h) & 95% (latest 3h) data (post-screening) availability</i>	yes
8	very good	<i>High quality, 95% (latest 1h) & 95% (latest 3h) data (post-screening) availability (lowest quality acceptable for operational alerts/warnings)</i>	yes
7	good	<i>95% (1h) & 75% (3h) input data (post-screening) availability</i>	yes
6	good	<i>75% (1h) & 75% (3h) input data (post-screening) availability (lowest quality acceptable for derivative products, eg. hybrid model)</i>	yes
5	fair	<i>75% (1h) & 66% (3h) input data (post-screening) availability</i>	yes
4	fair	<i>66% (1h) & 66% (3h) input data (post-screening) availability (lowest quality acceptable for post-processing purposes, eg. interpol.)</i>	yes
3	poor	<i>66% (1h) & 33% (3h) input data (post-screening) availability</i>	yes
2	poor	<i>33% (1h) & 33% (3h) input data (post-screening) availability</i>	yes
1	n/a (no assessment)	No quality assessment performed (gross deficiencies encountered in data screening and/or processing, eg. no data available from latest 1h or there is < 33% data in latest 3h) <i>(corresponding to K = -1)</i>	no
0	n/c (no calculations)	No calculations performed (severe technicalities encountered during data acquisition) <i>(corresponding to K = -1)</i>	no

Table II. Quality control flag (QCF) description with respect to data input, screening and processing.

It is clear that to use the nowcast value for the crucial alerts/warning sent to users, the nowcast should deliver a value of high quality (QCF ≥ 8), meaning that at least 95% of the latest dynamic 180-minute-long data record (95% from both the latest 60 and 180 minutes) is populated with “clean” magnetogram measurements. Similarly, to use the output for consecutive derivative products/services (e.g. in the hybrid model utilising ground- and space-based observations), the quality needs to be at least classified as “good” (QCF ≥ 6) meaning that at least 75% of the dynamic data record is available. The quality threshold acceptable for post-processing purposes, that may include interpolation of the values over the gaps, is set to 66% of the dynamic data record (“fair”, QCF ≥ 4). K nowcast values of “poor” quality (QCF < 2) are recorded only for statistical purposes. In case of severe technical problems encountered during data acquisition (QCF=0) and data screening/processing (QCF=1), K value is not produced (K is set to -1).

5. K index nowcast system at a single observation site - development

A nowcast system for real-time processing of geomagnetic field measurements, production of the local geomagnetic index K, and dissemination of the results has been developed. It has a complex, modular design (cf. **Fig.8**) aimed at timely data acquisition, fast production and distribution of the index value, while allowing for easy installation of further software developments. Key modules are the system control (incl. timing, quality, and communication), data acquisition (linked to IMF, the Instruments and Measurements Facility), database management, data processing (input screening/cleaning, actual K index calculation, post-processing), reference matrices (QC and LRC), communication display and dissemination. These modules are to be briefly outlined next.

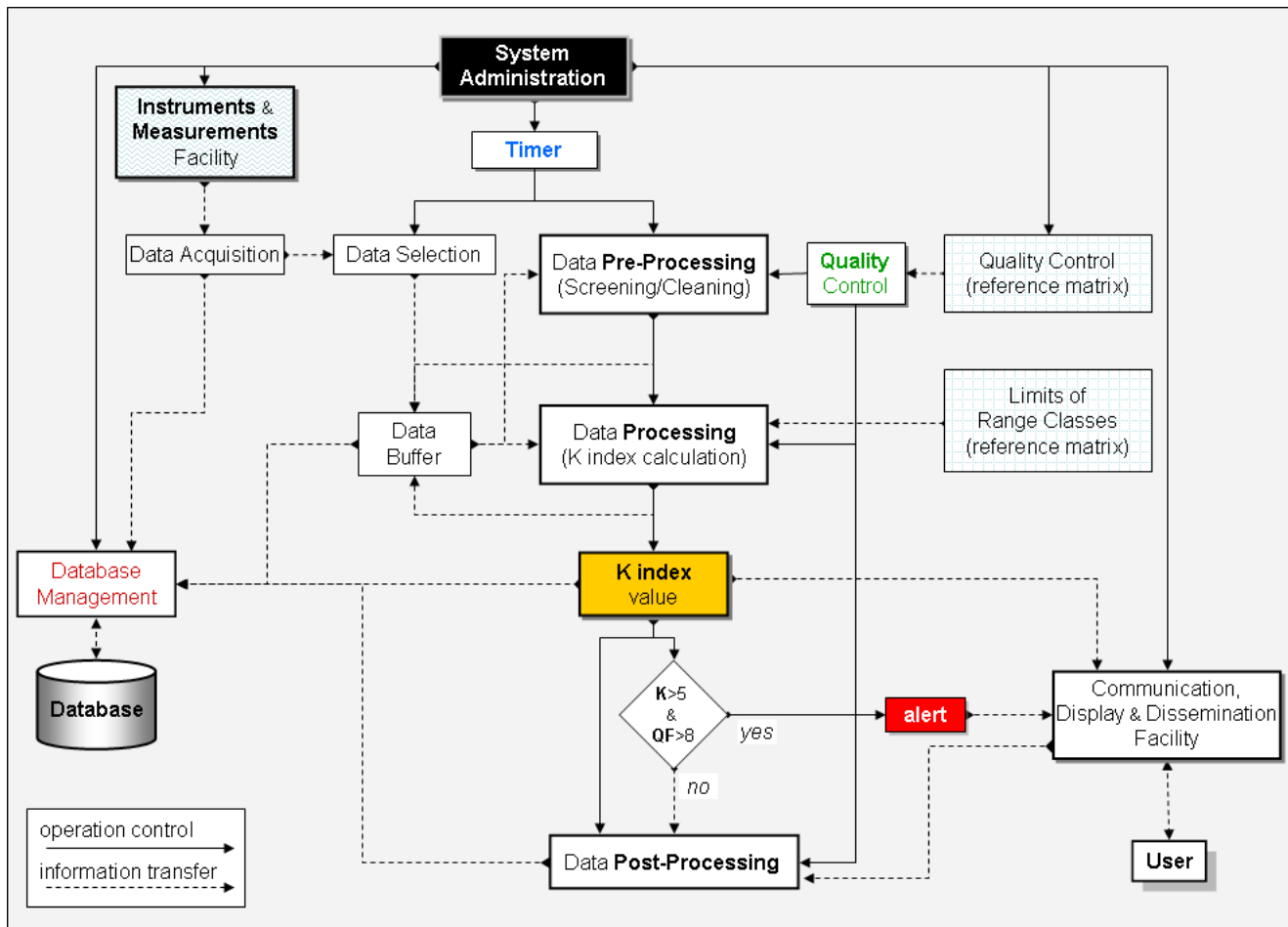


Fig.8. The K index nowcast/alert system layout.

This is a time-controlled system (rather than an event-driven system) producing a regular output (the K index value, data quality/processing evaluation, alerts) with certain time resolution. The current time resolution is set to 60 minutes and the data acquisition (from the last 60 minutes) and pre-processing phases are started immediately after the hour mark. Theoretically, the time resolution can be increased up to 1 minute (since we are using 1-min measurements records); however, such high resolution is not needed at the moment because user applications demanding such rate are not yet identified.

The data used in this study come primarily from observations carried out at the geomagnetic observatory in Dourbes, Belgium. The Dourbes observatory (IAGA code: DOU) started in 1953 following on the previous century-old tradition of magnetic observations in the Brussels area. Since 2002 the Dourbes observations have been digitally obtained and distributed via Intermagnet.

The key instrumentation set consists of variometers (2 systems currently in operation: fluxgate 3-axial and proton vector magnetometers) for measuring the variation of the field components about the baseline values and magnetometers for the absolute measurements needed to establish the values of the baselines. DI-flux magnetometers are used for absolute measurements of the declination (D) and inclination (I), while an Overhauser proton magnetometer is used for the total field (B) induction. Optical pumping potassium magnetometers are used for calibration purposes. The precision is 1 sec for time (with the potassium magnetometer), 0.1 nT for the induction, and 0.001° for the declination (and inclination). Here we use 1-min vector magnetic field (H, D, and Z components) data as obtained directly from the instruments, i.e. untreated, meaning that gaps and spikes are present in the input data set.

Given the pre-determined time resolution of the nowcast (currently 1 hour), the data acquisition module updates the data buffer with the measurements available since the last run. After that, the data pre-processing starts. It involves identification of data gaps and spurious values, providing information for quality control and update of the buffer with clean data. The main task of the data processing module is to compute the ranges (max-min) of the horizontal components, then select the largest one, and produce the K index value. All phases of the data processing are monitored closely by the QC system in order to immediately assess the quality of the data input and processing (based on the quality control reference matrix).

If the K value exceeds the threshold for a geomagnetic storm (K=5) and the dataset used for calculating K is of high quality (QF>8), an alert is generated and sent to the user. The alerts are some of the higher-level products generated by the system. Other products envisaged are the definitive K index (based on the linear elimination method) and various statistical analyses that may be requested by the user. These tasks are to be performed in the post-processing unit. Finally, it should be noted that all interaction with the user is done not directly but via the Communication Display and Dissemination (CDD) facility. In this way, the system is more flexible to respond adequately to the particular needs of different users.

6. K index nowcast system – assessment of performance

The performance of the K index nowcast has been tested in terms of efficiency in identifying and handling gaps/spurious/noisy input data plus the achieved accuracy of the output K index. The evaluation covered various levels of geomagnetic activity – from regular to extreme. A preliminary assessment of performance is presented here.

6.1 Evaluation – input dataset

For evaluation purposes, the nowcast process was simulated by feeding original 1-min digital magnetogram records (in blocks of 60) to the operational system and monitoring the production of the K index together with the corresponding QC flag. Digital magnetometer measurements data from Dourbes are available since year 2002 onwards, so we've had at our disposal an interrupted dataset for a period covering both high and low solar activity, with several geomagnetic storm events suitable for case studies. The nowcast-estimated index (K_{est}) was compared with the corresponding definitive values of K (K_{def}) to obtain the accuracy of the nowcast output. The definitive K index, used in the accuracy assessment, was produced at each year's end from manually-cleaned magnetogram records by utilising the method of adaptive smoothing (*Jankowski et al.*, 1988; *Nowozynski et al.*, 1991).

6.2 Evaluation - handling gaps/spurious data and technical problems

Here we assess how the nowcast system handles the most frequently occurring technicalities. In retrospect, many of the problems would be relatively easy to correct, for example to remove the spikes and/or to interpolate over the gaps if their size is small. However, in real time, the task is obviously much more complicated.

The data gaps are relatively easy to identify and process, unfortunately if the gap is longer than 3 hours, like in the presented case (**Fig.9A**), there is not much that the system can do about it apart from setting the quality flag to its lowest values, 1 or 2. In this case, an index value is not produced (K is set to -1) until the data flow recovered at 10:00UT. The K value production is resumed at the first opportunity (at 11:00UT) but due to missing data from the preceding couple of hours, the quality is qualified as poor so the QF is set to 2. The quality improves in time and by 14:00UT the estimated quality is already high ($QF=9$).

The next two cases (**Fig.9B,C** bottom panels) are more difficult to handle because there are mixtures of gaps, outliers and instances of plausible values, all occurring within a 3 hour interval. The situation is not helped by the obvious differences observed in the measurements of the two field components. Nevertheless, the procedure is able to successfully remove the outliers, and in the former case (**Fig.9B**), to even produce the correct K value at 14:00UT (**Fig.9B**, top panel); albeit the confidence is low so the QF is set to 3 (**Fig.9B**, middle panel). The next panel (**Fig.9D**) shows how the system processes the data during a rare technical problem that occurred in July 2009 affecting the measurements for an extended period of 3 days. Since human intervention may not be immediately possible to fix a technical problem at a certain observatory, the procedure should be able to immediately assess the situation and handle it according to the objectives. In this case, there are no gaps but data is extremely noisy, regular values frequently mixed with outliers of different magnitudes. The system was able to identify all outliers but because of the pre-set threshold on the max number, that can be removed from the input data set, a K value is still produced although it is incorrect and the quality flag immediately signals the degradation in quality. The system ignores such values and no alert/warning is dispatched in such situations.

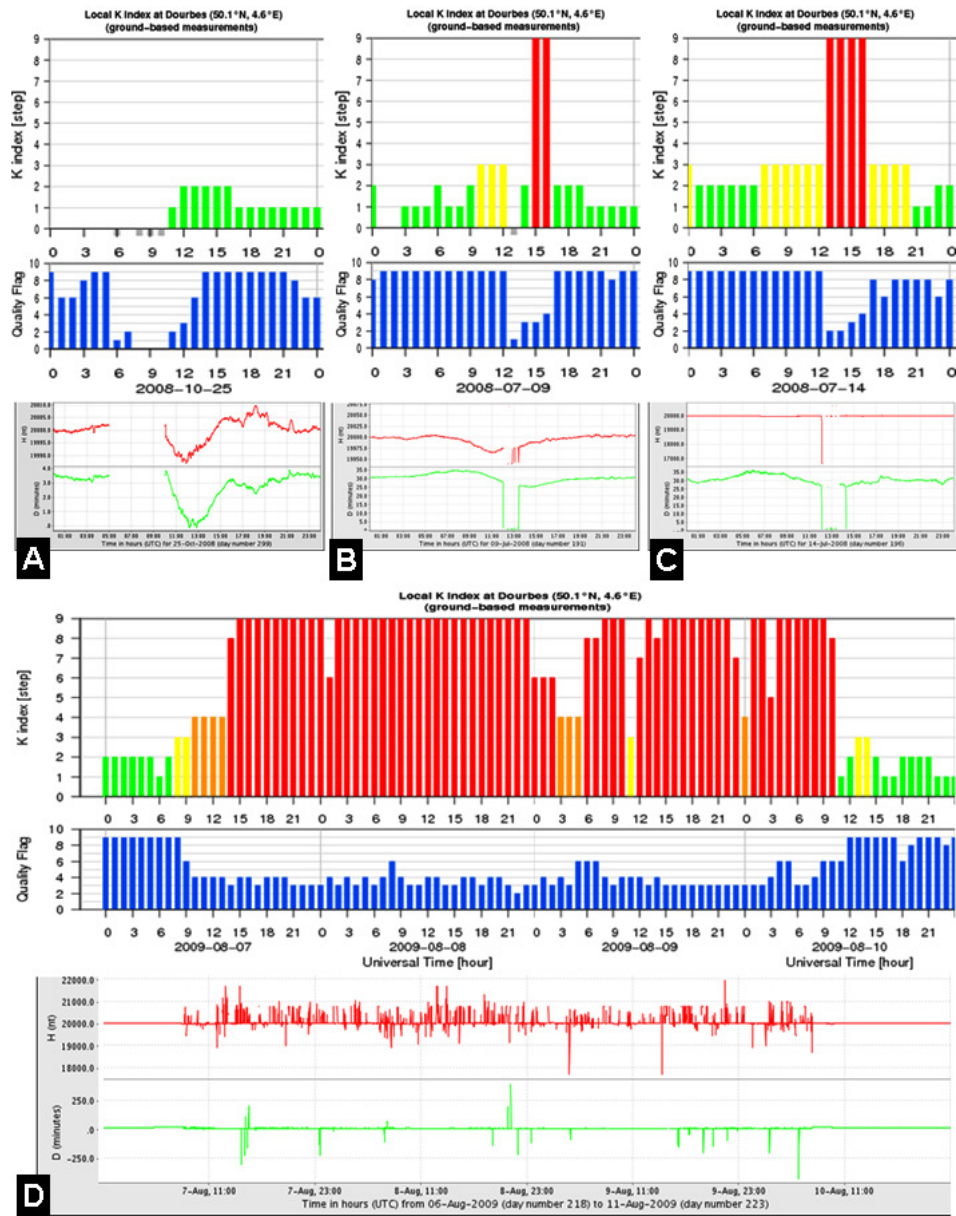


Fig.9. Nowcast system's handling spurious/noisy data and technicalities.

Again, it should be noted that the nowcast system is designed to operate autonomously, with little or no human intervention. In all cases, we rely on both the K value and the quality assessment (QF) to prepare alerts of ongoing disturbances/storms. The system performance is satisfactory in all situations experienced so far.

6.3 Evaluation – performance during geomagnetic disturbances

Presented next is the system evaluation during mild geomagnetic disturbances (**Fig.10**) and severe geomagnetic storms (**Fig.11**). These are arbitrary chosen events just to show the performance of the system. The results confirm that the nowcast is sensitive to even slight magnetic disturbances and correctly estimates the K value. The residual error is rarely exceeding 1 KU. On average, the error slightly increases during the major storm events.

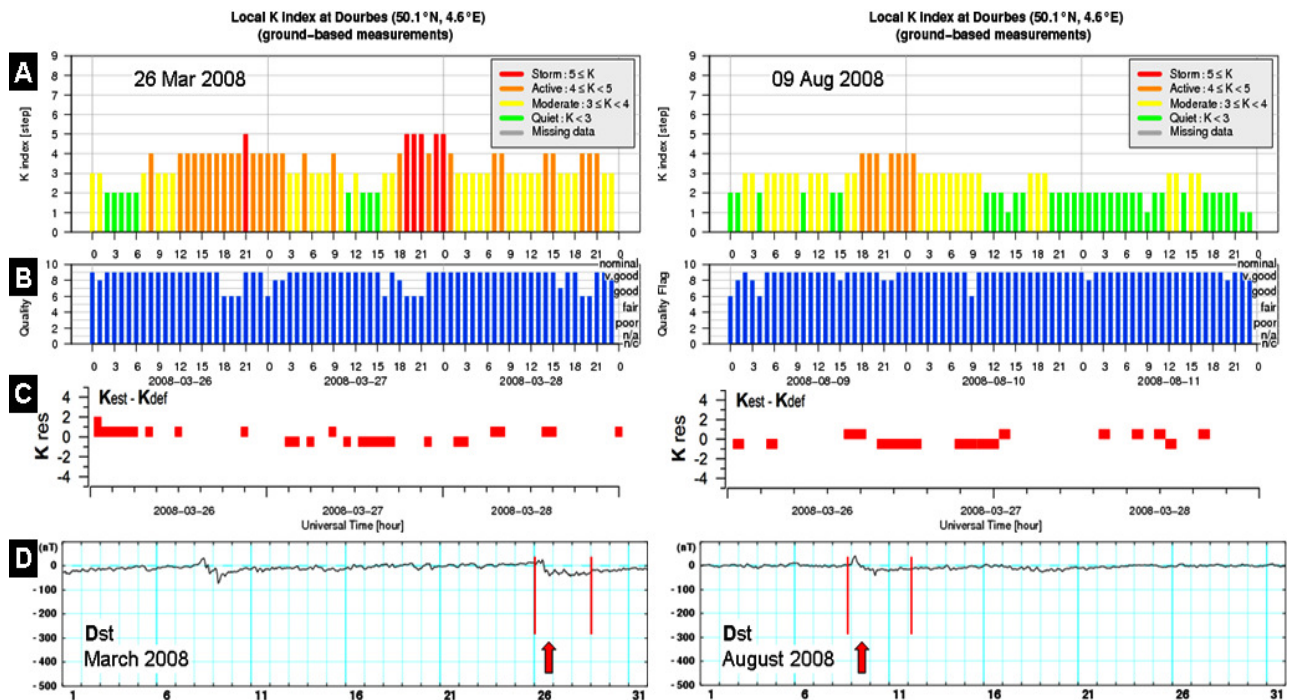


Fig.10. Exemplary results of K index operational production during recent minor geomagnetic events of increased geomagnetic activity. Panel (A): K index nowcast. (B): Quality flag. (C): Residual errors, nowcast (Kest) minus definitive (Kdef) values. (D): Dst index, for reference only.

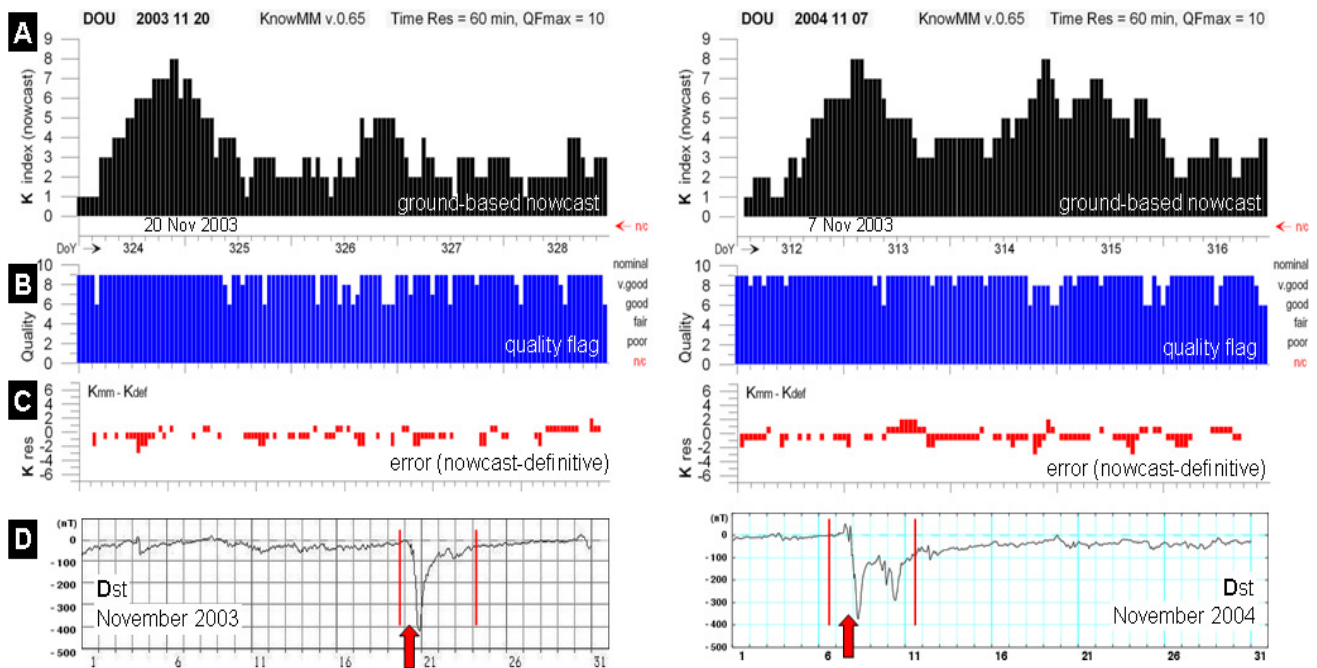


Fig.11. Evaluation results of the K index operational production during the major storm events in November 2003 and 2004. Panel (A): K index nowcast. (B): Quality flag. (C): Residual errors, nowcast (Kest) minus definitive (Kdef) values. (D): Dst index.

6.4 Evaluation – overall performance

We have calculated the residual error, i.e. the nowcast K (K_{est}) minus definitive K (K_{def}) value, over the entire period of available raw and definitive data (2002-2008, total data number 58727). The summarised results (**Fig.12**) show that almost 50% of the nowcast yields the correct K value and more than 90% of the total nowcast is within 1 KU difference from the correct, definitive value. The nowcast however, tends to overestimate the low geomagnetic activity values, and oppositely, to underestimate the high end of the geomagnetic activity.

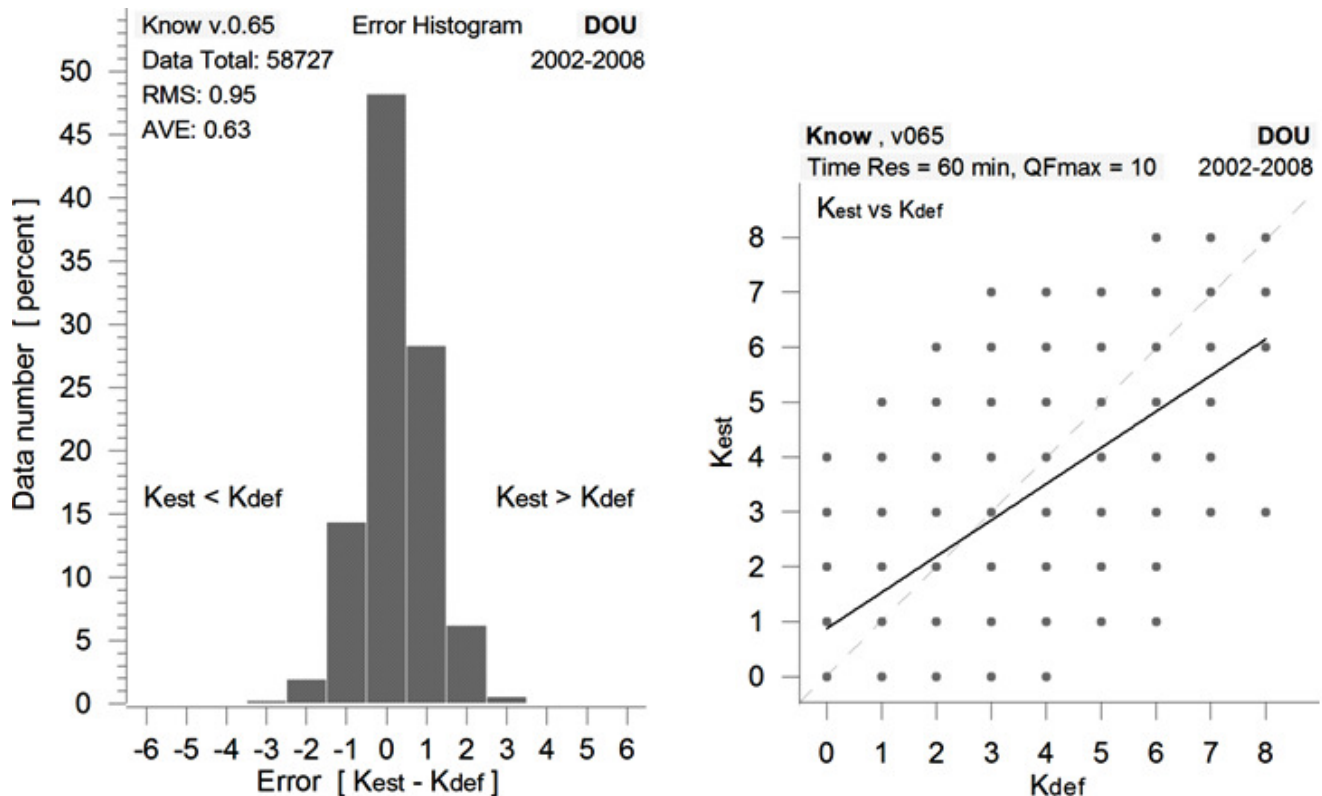


Fig.12. Evaluation results of the K index nowcast production over the period of 2002-2008. Left: Histogram of the residual errors, nowcast K (K_{est}) minus definitive K (K_{def}). Right: Scatter plot of nowcast K vs definitive K values.

The average residual error is estimated at about 0.63 and the RMS error is about 0.95 over the entire period, i.e. both estimates are less than 1 K unit. It should be noted that these errors may be due partly to the fact that K_{def} is calculated once over three hours (no overlapping of the time intervals), whereas K_{est} is calculated every one hour (albeit based on the latest three hours of data). Another contribution to the error is due to the use of QF=6 as the lowest threshold for inclusion in the statistical analysis, i.e. there is a probability of input data gaps (in the 3-hour intervals) as large as 25%.

6.5 Evaluation – impact of day-to-day variability

The definition of the standard K index implies that the day-to-day variability of the diurnal variation should also be accounted. As mentioned before, we assume that the diurnal variation is slowly changing from day to day, effectively considering it constant over a month-long period. This is another reason behind the occurrence of large Kest-Kdef residuals exceeding 2 KU. It is clearly a trade-off when estimating the index but we are prepared to accept it as it is not possible to directly apply the standard rules for the K index estimation in a real time procedure. To further investigate the issue, we have sorted the residuals with respect to season and local time. No particular seasonal or local time distribution of the large Kest-Kdef residuals is observed (**Fig.13**).

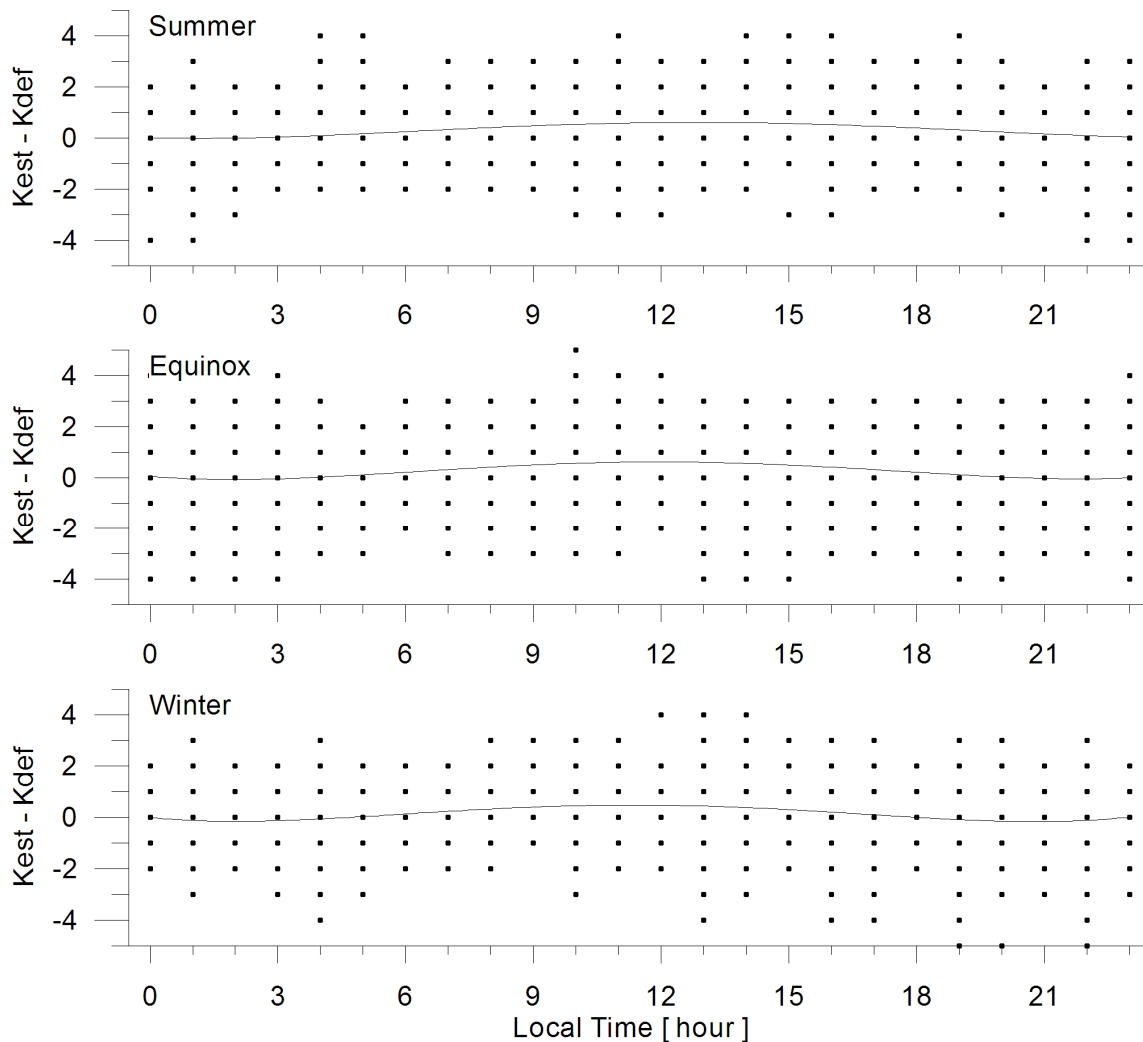


Fig.13. Evaluation results of the K index nowcast for the period of years 2002-2008, Dourbes. Seasonal and local time variations of the difference between the nowcast K (Kest) and definitive K (Kdef) values.

However; it is obvious that during daytime the nowcast tends to overestimate the K value. This overestimation is most substantial around noon when the average differences reaching about 0.6 units. The overestimation persists during all seasons and can be seen also in the error histogram (**Fig.12**).

7. Summary and Outlook

The space weather research community aim at developing reliable services for nowcasting and forecasting the ionospheric effects on the present-day technological systems (e.g. on GNSS-based applications) and a key component in these efforts is the nowcast and forecast of the geomagnetic activity. Also, a great variety of models rely on the traditional K indices as input parameters. However, the 3-hour time interval between the consecutive K index computations is now viewed as a serious obstacle considering that many phenomena are already known to exhibit shorter time constants. As a result, these indices have been targeted for further, high-time resolution developments. We offer here a K value every one hour using data from the preceding 3-hour window.

As mentioned in the previous sections, a clean data set is a pre-requisite for a high-quality calculation of the K value. Therefore, efficiently handling eventual technicalities is very important. Some of the problems can be solved easier if there is data from an observatory in close proximity. We have investigated the data set from another Belgian observatory (*Rasson, 2007*), Manhay (50.3°N, 5.7°E), and found that the simultaneous use of both data sets can improve the integrity of the nowcast service. The components ranges observed at these 2 stations are highly correlated so, if the main observatory used for the nowcast (Dourbes) is experiencing degradation in quality, the system can immediately verify (with the other station's data set) whether there is indeed a technical problem (**Fig.14**). Eventually, if the problem persists, it would be possible to replace the main input data with corresponding data from the other station. This approach would guarantee the service continuity/availability.

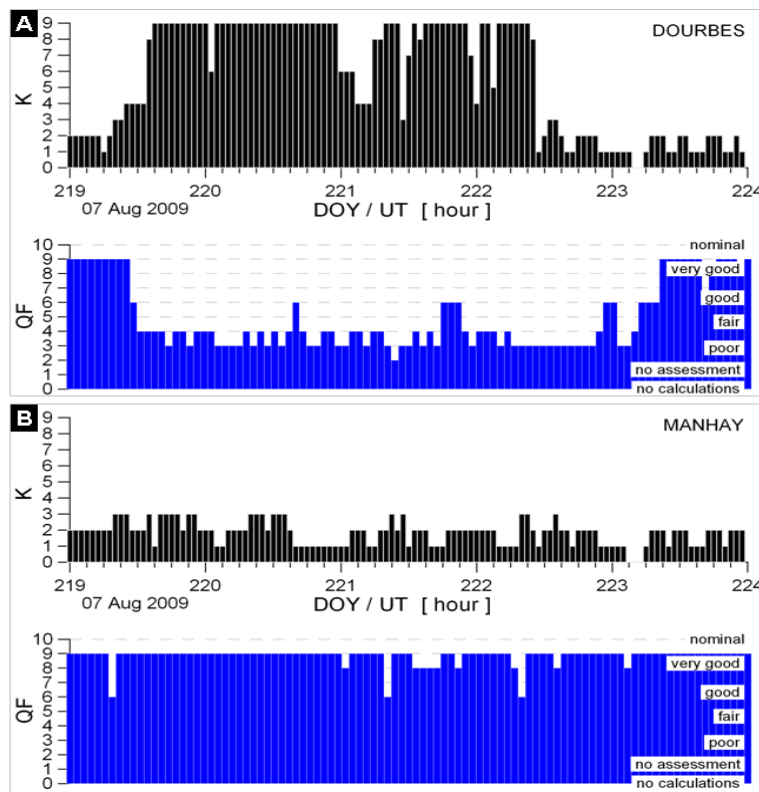


Fig.14. Comparison between the K index calculations at two observatories in a close distance, Dourbes (panel A) and Manhay (panel B).

Several methods of nowcasting and forecasting the geomagnetic indices, based on space-based observations of the solar wind, have recently been developed and will be used to further improve the here-presented nowcast service and the alerts module of the procedure.

The space-based estimate (K_{sw}) uses Advanced Composition Explorer (ACE) satellite data and an analogue model (MAK) relating the K_p index to solar wind parameters. The concept is based on the assumption that the geomagnetic index K (also, K_p) can be presented as a delayed reaction of the auroral ionosphere to the solar wind-magnetosphere interaction. A proxy index K_{sw} has been developed (*Andonov et al., 2004*), correlated with the ground-based K (K_p) index, i.e. $K_{sw} = a_0 + a_1 B_{zm} + a_2 P + a_3 V + a_4 (B_{zm})^2 + a_5 P^2$, where B_{zm} is the IMF B_z modified function, P is the solar wind dynamic pressure, and V is the solar wind velocity. The model uses measurements from the ACE satellite, performing measurements over a wide range of energies and nuclear masses, under all solar wind flow conditions.

In addition, a new, hybrid model for nowcasting/forecasting the geomagnetic K index has been developed based on the combined use of ground-based magnetic field measurements and solar-wind parameters, all data obtained in real time. The main idea of the hybrid approach consists (*Kutiev et al., 2009*) in calibration of the MAK values (K_{sw}) with the help of magnetogram-derived K index (K_{gnd}). The hybrid approach inherits the advantages of the space based concept with the robustness of the ground-based estimation of K . The overall prediction error is estimated at approximately 0.38 (in K units).

The Dst index, available in real time can be very useful in the alert system as it will provide additional reference/information on a storm development, e.g. the storm onset, beginning of the recovery phase, and its end.

Last but not least, the QCF matrix can further be elaborated to include the assessment of the recent nowcast accuracy, based on comparison with the “close to definitive” K value as soon as this value becomes available.

References

- Akasofu, S.I., Chapman, S., 1972. Solar-terrestrial physics. Clarendon Press, Oxford, 901 pp.
- Andonov, B., Muhtarov, P., Kutiev, I., 2004. Analogue model relating Kp index to solar wind parameters. *Journal of Atmospheric and Solar-Terrestrial Physics* 66(11), 927-932.
- Bartels, J., Heck, N.H., Johnson, H.F., 1939. The three-hour-range index measuring geomagnetic activity. *Terrestrial Magnetism and Atmospheric Electricity* 44, 411-454.
- Berthelier, A., Menvielle, M., Bitterly, M., 1996. Quasi real time determination of K-derived planetary indices - 1. The K index derivation. Proc. VIth International Workshop on geomagnetic observatory instruments, data acquisition and processing. 18-24 September 1994, Dourbes, Belgium, 144-147.
- Bevington, P.R., 1969. *Data Reduction and Error Analysis for the Physical Sciences*. McGraw-Hill, New York, NY, 336 pp.
- Bitterly, M., Menvielle, M., Bitterly, J., Berthelier, A., 1996. A Comparison Between Computer Derived (FMI Method) and Hand Scaled K Indices at Port aux Francais and Port Alfred French Observatories. Proc. VIth International Workshop on geomagnetic observatory instruments, data acquisition and processing. 18-24 September 1994, Dourbes, Belgium, pp.144-147.
- Burger, R.H., Sheehan, A.F., Jones, C.H., 2006. *Introduction to Applied Geophysics*. W.W.Norton and Co., New York, NY, 600 pp.
- Chapman, S., Bartels, J., 1940. *Geomagnetism*. Oxford University Press, London.
- Datta-Barua, S., Walter, T., Blanch, J., Enge, P., 2005. Can WAAS Availability Be Inferred From Geomagnetic Data? Proc. Ionospheric Effects Symposium 2005, 3-5 May 2005, Alexandria, VA.
- Della-Rose, D.J., Sojka, J.J., Zhu, L., 1999. Resolving geomagnetic disturbances using "K-like" geomagnetic indices with variable time intervals. *Journal of Atmospheric and Solar-Terrestrial Physics* 61, 1179-1194.
- Grubbs, F.E., 1969. Procedures for detecting outlying observations in samples. *Technometrics* 11(1), 1-21.
- Heitmeyer, C., Mandrioli, D., 1996. *Formal Methods for Real-Time Computing*. John Wiley, New York, NY, 225 pp.
- Hopgood, P.A., 1986. On the computer generation of geomagnetic K-indices from digital data. *Journal of Geomagnetism and Geoelectricity* 38(9), 861-871.
- Knecht, D.J., 1972. The geomagnetic field. *Air Force Surveys in Geophysics*, No. 246, Report No. AFCRL-72-0570, Air Force Cambridge Research Laboratories, Bedford, MA, 120 pp.
- Kohl, H., Rüster, R., Schlegel, K., (Ed.), 1996. *Modern Ionospheric Science*. European Geophysical Society, Katlenburg-Lindau, 346-370.
- Jacobs, J.A., 1987. *Geomagnetism*. Volumes 1 (627 pp.), 2 (579 pp.), and 3 (533 pp.) Academic Press Ltd.
- Jankowski, J.A., Ernst, T., Sucksdorff, C., Pirjola, R., Ryno, J., 1988. Experiences of a filter method and a standard curve method for determining K-indices. *Annales Geophysicae* 6(6), 589-594.
- Jankowski, J.A., Sucksdorff, C., 1996. *IAGA Guide for Magnetic Measurements and Observatory Practice*. IAGA / NOAA Space Environment Center, Boulder CO, 235 pp.
- Jodogne, J.C., Stankov, S.M., 2002. Ionosphere-plasmasphere response to geomagnetic storms studied with the RMI-Dourbes comprehensive database. *Annals of Geophysics* 45(5), 629-647.
- Kutiev, I., Muhtarov, P., Andonov, B., Warnant, R., 2009. Hybrid model for nowcasting and forecasting the K index. *Journal of Atmospheric and Solar-Terrestrial Physics* 71, 589-596.
- Mayaud, P.N. (1967). *Atlas des indices K*, IAGA Bull. 21, Int. Union of Geod. and Geophys., Paris.

- Mayaud, P.N., 1980. Derivation, meaning and use of geomagnetic indices. Geophysical Monograph Series 22, AGU, Washington, DC, 154 pp.
- Mellichamp, D.A., 1983. Real-time computing with applications to data acquisition and control. Van Nostrand, New York, NY, 552 pp.
- Mendes, O., Domingues, M.O., Mendes da Costa, A., Clua de Gonzalez, A.L., 2005. Wavelet analysis applied to magnetograms: singularity detections related to geomagnetic storms. *Journal of Atmospheric and Solar-Terrestrial Physics* 67, 1827-1836.
- Menvielle, M., 1990. About the derivation of geomagnetic indices from digital data. In: Kauristie, K., Sucksdorff, C., Nevanlinna, H., (Ed.), *Proc. International Workshop on Observatory Data Acquisition and Processing*, Geophysical Publications N°15, Finnish Meteorological Institute, Helsinki, 117-126.
- Menvielle, M., Berthelier, A., 1991. The K-derived planetary indices: description and availability. *Reviews of Geophysics* 29(3), 415-432.
- Menvielle, M., Papitashvili, N., Hakkinen, L., Sucksdorff, C., 1995. Computer production of K indices: review and comparison of methods. *Geophysical Journal International* 123(3), 866-886.
- Niblett, E.R., Loomer, E.I., Coles, R., Jansen Van Beek, G., 1984. Derivation of K indices using magnetograms constructed from digital data. *Geophysical Surveys*, 6(3-4), 431-437.
- Nowozynski, K., Ernst, T., Jankowski, J.A., 1991. Adaptive smoothing method for computer derivation of K-indices. *Geophysical Journal International* 104, 85-93.
- Olsen, N, Hulot, G., Sabaka, T.J., 2007. The Present Field. In: *Treatise of Geophysics, Geomagnetism*, v.5, (Kono, M., editor), Elsevier, 33-75.
- Pirjola, R., Ryno, J., Sucksdorff, C., 1990. Computer production of K-indices by a simple method based on linear elimination. In: Kauristie, K., Sucksdorff, C., Nevanlinna, H., (Ed.), *Proc. International Workshop on Observatory Data Acquisition and Processing*, Geophysical Publications N°15, Finnish Meteorological Institute, Helsinki, 136-146.
- Rasson, J.L., 2007. Observatories in Benelux countries. In: Gubbins, D., Herrero-Bervera, E., (Ed.), *Encyclopedia of Geomagnetism and Paleomagnetism*, Springer, pp.725-726.
- Riddick, J.C., Stuart, W.F., 1984. The generation of K-indices from digitally recorded magnetic data. *Geophysical Surveys* 6(3-4), 439-456.
- Schultz, A., Zhang, T., 1990. Exorcise—an algorithm for detection of spurious values and prediction of missing data. *Computers & Geosciences* 16(8), 1027-1065.
- Siebert, M., 1996. Geomagnetic activity indices. In: Dieminger, W., Hartmann, G.K., Leitinger, R., (Ed.), *The Upper Atmosphere – Data Analysis and Interpretation*, Springer, Berlin, pp. 887-911.
- Snedegor, G.W., Cochran, W.G., 1980. *Statistical Methods* (7-th edn). Iowa State University Press, Ames IA, 507 pp.
- Stankov, S.M., Jakowski, N., Heise, S., Muhtarov, P., Kutiev, I., Warnant, R., 2003. A new method for reconstruction of the vertical electron density distribution in the upper ionosphere and plasmasphere. *Journal of Geophysical Research* 108(A5), 1164, doi:10.1029/2002JA009570.
- Stankov, S.M., Kutiev, I.S., Jakowski, N., Wehrenpfennig, A., 2004. GPS TEC forecasting based on auto-correlation analysis. *Acta Geodaetica et Geophysica Hungarica* 39(1), 1-14.
- Stankov, S.M., Jakowski, N., Tsybulya, K., Wilken, V., 2006. Monitoring the generation and propagation of ionospheric disturbances and effects on GNSS positioning. *Radio Science* 41(5), RS6S09.
- Stankov, S.M., Jakowski, N., 2007. Ionospheric effects on GNSS reference network integrity. *Journal of Atmospheric and Solar-Terrestrial Physics* 69(4-5), 485–499.
- Stankov, S.M., Warnant, R., Stegen, K., 2009. Trans-ionospheric GPS signal delay gradients observed over mid-latitude Europe during the geomagnetic storms of October-November 2003. *Advances in Space Research* 43(9), 1314-1324.

- Sucksdorff, C., Pirjola, R., Häkkinen, L., 1991. Computer production of K-indices based on linear elimination. *Geophysical Transactions* 36(3-4), 335-345.
- Swaroop, R., 1971. A statistical technique for computer identification of outliers in multivariate data. NASA Technical Note D-6472, NASA Washington DC, August 1971, 29 pp.
- Takahashi, K., Toth, B.A., Olson, J.V., 2001. An automated procedure for near-real-time Kp estimates. *Journal of Geophysical Research* 106, 21017-21032.
- Van Wijk, A.M., Nagtegaal, D., 1977. K measurements by computer. *Journal of Atmospheric and Terrestrial Physics* 39, 1447-1450.
- Viljanen, A., Pulkkinen, A., Pirjola, R., 2008. Prediction of the geomagnetic K index based on its previous value. *Geophysica* 44(1-2), 3-14.
- Walker, J.K., 1987. Adaptive separation of regular and irregular magnetic activity for K indices. *Journal of Atmospheric and Terrestrial Physics* 49, 1017-1025.
- Warnant, R., Lejeune, S., Bavier, M., 2007a. Space Weather influence on satellite based navigation and precise positioning. In: Liliensten, J. (Ed.) *Space Weather - Research towards Applications in Europe*, Astrophysics and Space Science Library series, Vol. 344, Springer, pp. 129-146.
- Warnant, R., Kutiev, I., Marinov, P., Bavier, M., Lejeune, S., 2007b. Ionospheric and geomagnetic conditions during periods of degraded GPS position accuracy: 1. Monitoring variability in TEC which degrades the accuracy of Real Time Kinematic GPS applications. *Advances in Space Research* 39(5), 875-880.
- Warnant, R., Kutiev, I., Marinov, P., Bavier, M., Lejeune, S., 2007c. Ionospheric and geomagnetic conditions during periods of degraded GPS position accuracy: 2. RTK events during disturbed and quiet geomagnetic conditions. *Advances in Space Research* 39(5), 881-888.
- Wilson, L.R., 1987. An evaluation of digitally derived K-indices. *Journal of Geomagnetism and Geoelectricity* 39, 97-109.
- Wing, S., Johnson, J.R., Jen, J., Meng, C.-I., Cibeck, D.G., Bechtold, K., Freeman, J., Costello, K., Balikhin, M., Takahashi, K., 2005. Kp forecast models. *Journal of Geophysical Research* 110, A04203, doi: 10.1029/2004JA010500.



STR-RMI-2010-01	Unclassified	Version: 1.1 / 01.10.2010	Page: 32 / 32
Title:	Local operational geomagnetic index K calculation (K-LOGIC) from digital ground-based magnetic measurements		

END OF DOCUMENT